Evolution of light-current characteristic shape in high-power semiconductor quantum well lasers

Z.N. Sokolova, N.A. Pikhtin and L.V. Asryan✉

The light-current characteristic (LCC) of semiconductor quantum well lasers is theoretically studied. It is discussed here that, due to internal optical absorption loss, which depends on the electron and hole densities in the optical confinement layer, (i) roll-over of the LCC occurs with increasing injection current, and, (ii) depending on the parameters of laser structures, the LCC can have two branches, i.e. the optical emission at two different output powers will be possible within a certain range of injection currents.

Introduction: We develop a theory of light-current characteristic (LCC) of semiconductor quantum well (QW) lasers (Fig. 1) in the presence of internal optical absorption loss, which depends on the carrier density in the optical confinement layer (OCL) [1]. We show that, depending on the parameters of laser structures, one of the following two situations will be realised:

(i) Roll-over of the LCC occurs with increasing injection current, i.e. the output power first increases, approaches its maximum value, and then decreases and continuously goes to zero at a certain current, which is the maximum operating current (Fig. 2, curves 1 and 2).
(ii) As in case (i), roll-over of the LCC occurs with increasing injection current. However, in contrast to case (i), the lasing quenches at a non-vanishing output power, i.e. while the output power is non-zero at the maximum operating current, there will be no lasing immediately beyond this point. In this case, in addition to the rolling-over branch of the LCC, there will be the second branch of the LCC, i.e. the second mode of lasing. The threshold for the second branch is higher than that for the first (conventional) branch and the maximum operating current is the same as that for the first branch (Fig. 2, curves 3 and 4). With increasing injection current from the second threshold to the maximum operating current, the output power of the second mode increases from zero and approaches the same value as that of the first mode, i.e. the two branches merge together (Fig. 2, curves 3 and 4). As in the first mode, there can be no lasing in the second mode beyond this merging point. Hence, in this case, above the second lasing threshold and up to the maximum operating current, there are two possible modes for lasing, i.e. the LCC is two-valued.

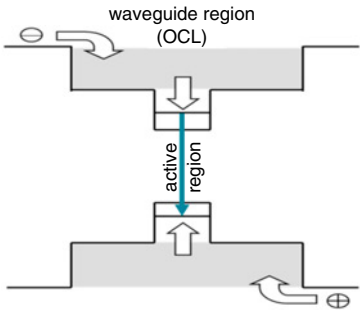

Fig. 1 *Schematic energy band diagram of a semiconductor laser with a low-dimensional active region*

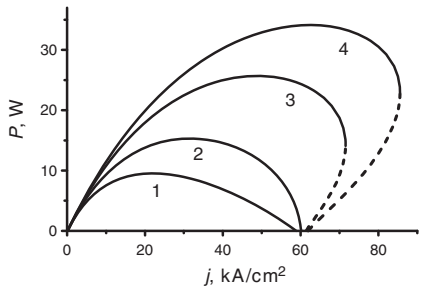

Fig. 2 *LCCs of QW laser structures or $v_{n,capt,0}$ ($\times 10^5$, cm/s): 1–5, 2–7.5, 3–10, 4–20; $v_{p,capt,0}$ ($\times 10^5$, cm/s): 1–3, 2–5, 3, 4–10*

In this work, we discuss the evolution of the LCC shape from the conventional rolled-over one [the above case (i)] to the two-valued one [case (ii)], which occurs with varying the QW laser structure parameters.

Theoretical model: Our model is based on the following set of five steady-state rate equations [2–4]:

for electrons in the OCL of thickness b $\left[b(\partial n^{\mathrm{OCL}}/\partial t)=0\right]$,

$$\frac{j}{e}+N_{\mathrm{QW}}\frac{n^{\mathrm{QW}}}{\tau_{n,\mathrm{esc}}}-N_{\mathrm{QW}}v_{n,\mathrm{capt},0}(1-f_n)\,n^{\mathrm{OCL}}-bB_{3\mathrm{D}}n^{\mathrm{OCL}}p^{\mathrm{OCL}}=0, \tag{1}$$

for holes in the OCL $\left[b(\partial p^{\mathrm{OCL}}/\partial t)=0\right]$,

$$\frac{j}{e}+N_{\mathrm{QW}}\frac{p^{\mathrm{QW}}}{\tau_{p,\mathrm{esc}}}-N_{\mathrm{QW}}v_{p,\mathrm{capt},0}(1-f_p)p^{\mathrm{OCL}}-bB_{3\mathrm{D}}n^{\mathrm{OCL}}p^{\mathrm{OCL}}=0, \tag{2}$$

for electrons in QWs $\left(\partial n^{\mathrm{QW}}/\partial t=0\right)$,

$$v_{n,\mathrm{capt},0}\,(1-f_n)\,n^{\mathrm{OCL}}-\frac{n^{\mathrm{QW}}}{\tau_{n,\mathrm{esc}}}-B_{2\mathrm{D}}n^{\mathrm{QW}}p^{\mathrm{QW}}-c_{\mathrm{g}}g^{\max}(f_n+f_p-1)\frac{N}{S}=0, \tag{3}$$

for holes in QWs $\left(\partial p^{\mathrm{QW}}/\partial t=0\right)$,

$$v_{p,\mathrm{capt},0}(1-f_p)p^{\mathrm{OCL}}-\frac{p^{\mathrm{QW}}}{\tau_{p,\mathrm{esc}}}-B_{2\mathrm{D}}n^{\mathrm{QW}}p^{\mathrm{QW}}-c_{\mathrm{g}}g^{\max}(f_n+f_p-1)\frac{N}{S}=0, \tag{4}$$

for photons in the lasing mode $\left(\partial N/\partial t=0\right)$,

$$c_{\mathrm{g}}N_{\mathrm{QW}}\,g^{\max}(f_n+f_p-1)N-c_{\mathrm{g}}(\beta+\alpha_{\mathrm{int}})N=0. \tag{5}$$

The following quantities are the five unknowns to be found from the solution of (1)–(5): n^{OCL} and p^{OCL} are the densities of electrons and holes in the OCL, n^{QW} and p^{QW} are the densities of electrons and holes in the QWs, and N is the number of photons of stimulated emission.

In (1)–(5), f_n and f_p are the occupancies of the states corresponding to the lower edge of the electron subband and to the upper edge of the hole subband in a QW. They are related to the electron and hole densities n^{QW} and p^{QW} in the QWs as follows [5–7]:

$$f_n=1-\exp\left(-n^{\mathrm{QW}}/N_{\mathrm{c}}^{2\mathrm{D}}\right),\quad f_p=1-\exp\left(-p^{\mathrm{QW}}/N_{\mathrm{v}}^{2\mathrm{D}}\right), \tag{6}$$

where $N_{\mathrm{c,v}}^{2\mathrm{D}}=m_{e,\,\mathrm{hh}}^{\mathrm{QW}}T/(\pi\hbar^2)$ are the 2D effective densities of states in the conduction and valence bands in the QWs, $m_{e,\,\mathrm{hh}}^{\mathrm{QW}}$ are the electron and hole effective masses in the QWs, and T is the temperature in units of energy.

The following parameters enter into (1)–(5): j is the injection current density, e is the electron charge, N_{QW} is the number of QWs, $v_{n,\mathrm{capt},0}$ and $v_{p,\mathrm{capt},0}$ are the capture velocities (measured in cm/s) of electrons and holes from the OCL, respectively, into an empty (at $f_n=0$ and $f_p=0$) QW, $\tau_{n,\mathrm{esc}}$ and $\tau_{p,\mathrm{esc}}$ are the thermal escape times of electrons and holes, respectively, from the QWs to the OCL which can be expressed in terms of the capture velocities – see [8, 9], $B_{3\mathrm{D}}$ and $B_{2\mathrm{D}}$ are the spontaneous radiative recombination coefficients in the bulk region (OCL) and 2D region (QWs) measured in cm^3/s and cm^2/s, respectively, (see [10, 11] for the expressions for $B_{3\mathrm{D}}$ and $B_{2\mathrm{D}}$), c_{g} is the group speed of light, $g^{\max}$ is the maximum modal gain in each QW (see [12] for the expression for $g^{\max}$), $S=WL$, where W is the stripe contact width and L is the cavity length, the mirror loss $\beta=(2L)^{-1}\,(R_1R_2)^{-1}$.

$\ln(R_1R_2)^{-1}$, R_1 and R_2 are the mirror reflectivities, and α_{int} is the internal optical absorption loss coefficient.

As seen from Fig. 1, the carriers are not directly injected into a quantum-confined active region of the laser. They are first injected from the cladding layers into the OCL and then they are captured from the OCL into the active region. A key component of our theoretical model is that we do not assume instantaneous capture of carriers from the OCL into the QWs, i.e. we do not assume that the capture velocities are infinitely high; instead, we use finite values for them. In fact, the capture velocities $v_{n,\mathrm{capt},0}$ and $v_{p,\mathrm{capt},0}$ may vary in different laser structures as they depend on the QW depth, i.e. on the compositions of the QW and OCL materials; they also depend on the QW width. In [13, 14], we evaluated the electron capture velocity for our experimental laser structures using our theoretical model.

Another key component of our theoretical model is the internal optical absorption loss, which depends on the electron and hole densities in the OCL [15]

$$\alpha_{\text{int}} = \alpha_0 + \Gamma^{\text{OCL}}\sigma_{n,\text{ int}}\, n^{\text{OCL}} + \Gamma^{\text{OCL}}\sigma_{p,\text{ int}}\, p^{\text{OCL}}, \quad (7)$$

where $\sigma_{\text{n,int}}$ and $\sigma_{p,\text{int}}$ are the cross sections of light absorption by electrons and holes in the OCL, respectively, Γ^{OCL} is the optical confinement factor in the OCL, and a_0 is the constant component of the internal loss coefficient, which is primarily due to light absorption in the cladding layers.

Owing to the fact that the carrier capture from the OCL into the QWs is not instantaneous, the densities of these carriers in the OCL are not pinned – they grow with increasing injection current in the lasing mode [16, 17]. As a result of this, as seen from (7), the internal optical loss in the OCL increases as well.

In contrast to [5, 6, 18], wherein charge neutrality was assumed to hold locally in a low-dimensional active region of the laser, we use here the condition of global charge neutrality, i.e. the condition of equality of the total charge of electrons in the OCL and QWs to the total charge of holes in these two regions [2–4]

$$e(N_{\text{QW}}n^{\text{QW}} + bn^{\text{OCL}}) = e(N_{\text{QW}}p^{\text{QW}} + bp^{\text{OCL}}). \quad (8)$$

The output optical power as a function of the injection current density (the LCC) is given as [19]

$$P(j) = \hbar\,\omega\, c_{\text{g}}\beta\, N(j), \quad (9)$$

where ω is the angular frequency of the lasing emission and $N(j)$ is the number of photons in the lasing mode, which is found from the solution of the set of rate equations (1)–(5).

In [18], under the condition of local charge neutrality in the active region, closed-form solutions of the rate equations were obtained and the following analytical criterion for the appearance of the second branch of the LCC was derived

$$\frac{\sigma_{n,\text{int}}v_{n,\text{capt},0}}{2bB_{3\text{D}}g^{\max}} > 1. \quad (10)$$

Under the condition of global charge neutrality in a QW laser structure, no closed-form solutions of the set of rate equations (1)–(5) can be obtained and, correspondingly, no analytical criterion for the appearance of the second branch of the LCC can be derived. However, the analytical criterion (10) proved to be helpful also in this case.

Discussion: We solve numerically the set of rate equations (1)–(5) for the experimental laser heterostructures emitting at 1.01 μm. A single strained QW of 50 Å width is made of indium gallium arsenide (InGaAs). The material of the OCL is GaAs, and the OCL thickness is $b = 1.7$ μm. The material of the cladding layers is $Al_{0.3}Ga_{0.7}As$. The cavity length is $L = 0.15$ cm. The cross-sections of light absorption by electrons and holes in the OCL are $\sigma_{n,\text{ int}} = 3 \times 10^{-18}$ cm^2 and $\sigma_{p,\text{int}} = 10^{-17}$ cm^2. The dopant concentrations in the n- and p-claddings are 5×10^{17} and 3.5×10^{18} cm^{-3}, respectively. The constant component of the internal loss coefficient is $\alpha_0 = 2$ cm^{-1}. The spontaneous radiative recombination coefficient in the OCL material (GaAs) is $B_{3\text{D}} = 2.044 \times 10^{-10}$ cm^3/s. The maximum modal gain is $g^{\max} = 51.89$ cm^{-1}.

Fig. 2 shows the LCCs calculated at various values of the electron and hole capture velocities from the OCL into the QW. Curve 1 corresponds to $v_{n,\text{capt},0} = 5 \times 10^5$ cm/s and $v_{p,\text{capt},0} = 3 \times 10^5$ cm/s; curve 2 corresponds to $v_{n,\text{capt},0} = 7.5 \times 10^5$ cm/s and $v_{p,\text{capt},0} = 5 \times 10^5$ cm/s; curve 3 corresponds to $v_{n,\text{capt},0} = 10^6$ cm/s and $v_{p,\text{capt},0} = 10^6$ cm/s; curve 4 corresponds to $v_{n,\text{capt},0} = 2 \times 10^6$ cm/s and $v_{p,\text{capt},0} = 10^6$ cm/s. As seen from Fig. 2, the LCC shape changes with varying the capture velocities. At relatively low capture velocities (curves 1 and 2), case (i) is realised, i.e. the output power increases, approaches its maximum value, and then decreases and continuously goes to zero. As also seen from the figure, the maximum output optical power increases with increasing capture velocities.

At high capture velocities (curves 3 and 4 in Fig. 2), case (ii) is realised, i.e. in addition to the rolling over (conventional) branch of the LCC, the second branch appears in the LCC. The threshold for the second branch is higher than that for the first branch. At the maximum operating current, the two branches merge together. Immediately beyond the merging point (at which the optical power is non-zero), there can be no lasing in the structure.

Conclusions: The LCC of semiconductor QW lasers has been theoretically studied in the presence of internal optical absorption loss, which depends on the electron and hole densities in the OCL. It has been shown that depending on the values of the electron and hole capture velocities from the OCL into the QW, two different shapes of the LCC can be realised. At low capture velocities, the LCC is single-branched and rolling over with increasing injection current. At high capture velocities, the LCC is two-branched – it has the second branch in addition to the rolling over branch. In contrast to the rolling over branch, the optical power in the second branch is continuously increasing with increasing pump current. The two branches merge together at the maximum operating current beyond which the lasing quenches in both branches.

Acknowledgments: This work was supported by the federal program of the Ioffe Institute. L.V. Asryan also thanks the U.S. Army Research Office (grant no. W911NF-17-1-0432) for support of this work.

Submitted: *16 January 2019* E-first: *25 March 2019*
doi: 10.1049/el.2019.0225
One or more of the Figures in this Letter are available in colour online.

Z.N. Sokolova and N.A. Pikhtin (*Ioffe Institute, St. Petersburg 194021, Russia*)

L.V. Asryan (*Virginia Polytechnic Institute and State University, Blacksburg, Virginia 24061, USA*)

✉ E-mail: asryan@vt.edu

References

1 Sokolova, Z.N., Pikhtin, N.A., and Asryan, L.V.: 'Two-valued characteristics in semiconductor quantum well lasers', *J. Lightwave Technol.*, 2018, **36**, (11), pp. 2295–2300
2 Sokolova, Z.N., Pikhtin, N.A., Tarasov, I.S., *et al.*: 'Theory of operating characteristics of a semiconductor quantum well laser: inclusion of global electroneutrality in the structure', *J. Phys. Conf. Ser.*, 2016, **740**, p. 012002
3 Sokolova, Z.N., Pikhtin, N.A., Tarasov, I.S., *et al.*: 'Threshold characteristics of a semiconductor quantum-well laser: inclusion of global electroneutrality in the structure', *Quantum Electron.*, 2016, **46**, (9), pp. 777–781
4 Sokolova, Z.N., Veselov, D.A., Pikhtin, N.A., *et al.*: 'Increase in the internal optical loss with increasing pump current and the output power of quantum well lasers', *Semiconductors*, 2017, **51**, (7), pp. 959–964
5 Asryan, L.V, and Luryi, S.: 'Two lasing thresholds in semiconductor lasers with a quantum-confined active region', *Appl. Phys. Lett.*, 2003, **83**, (26), pp. 5368–5370
6 Asryan, L.V, and Luryi, S.: 'Effect of internal optical loss on threshold characteristics of semiconductor lasers with a quantum-confined active region', *J. Quant. Electron.*, 2004, **40**, (7), pp. 833–843
7 Vahala, K.J., and Zah, C.E.: 'Effect of doping on the optical gain and the spontaneous noise enhancement factor in quantum well amplifiers and lasers studied by simple analytical expressions', *Appl. Phys. Lett.*, 1988, **52**, pp. 1945–1947
8 Asryan, L.V., and Sokolova, Z.N.: 'Optical power of semiconductor lasers with a low-dimensional active region', *J. Appl. Phys.*, 2014, **115**, p. 023107
9 Han, D.-S., and Asryan, L.V.: 'Output power of a double tunneling-injection quantum dot laser', *Nanotechnology*, 2010, **21**, (1), p. 015201
10 Asryan, L.V., and Suris, R.A.: 'Inhomogeneous line broadening and the threshold current density of a semiconductor quantum dot laser', *Semicond. Sci. Technol.*, 1996, **11**, (4), pp. 554–567
11 Asryan, L.V.: 'Spontaneous radiative recombination and nonradiative Auger recombination in quantum-confined heterostructures', *Quantum Electron.*, 2005, **35**, (12), pp. 1117–1120
12 Sokolova, Z.N., Tarasov, I.S., and Asryan, L.V.: 'Capture of charge carriers and output power of a quantum well laser semiconductors', *Semiconductors*, 2011, **45**, (11), pp. 1494–1500
13 Sokolova, Z.N., Bakhvalov, K.V., Lyutetskiy, A.V., *et al.*: 'Method for determination of capture velocity of charge carriers into quantum well in semiconductor laser', *Electron. Lett.*, 2015, **51**, (10), pp. 780–782
14 Sokolova, Z.N., Bakhvalov, K.V., Lyutetskiy, A.V., *et al.*: 'Dependence of the electron capture velocity on the quantum-well depth in semiconductor lasers', *Semiconductors*, 2016, **50**, (5), pp. 667–670

15 Casey, H.C., and Panish, M.B.: 'Heterostructure laser' (Academic Press, New York, 1978)
16 Asryan, L.V., Luryi, S., and Suris, R.A.: 'Intrinsic nonlinearity of the light–current characteristic of semiconductor lasers with a quantum-confined active region', *Appl. Phys. Lett.*, 2002, **81**, (12), pp. 2154–2156
17 Asryan, L.V., Luryi, S., and Suris, R.A.: 'Internal efficiency of semiconductor lasers with a quantum-confined active region', *J. Quantum Electron.*, 2003, **39**, (3), pp. 404–418
18 Asryan, L.V.: Unpublished
19 Agrawal, G.P., and Dutta, N.K.: 'Long-wavelength semiconductor lasers' (Van Nostrand, New York, 1986)